JATIS Journal of Astronomical Telescopes, Instruments, and Systems

RESEARCH PAPER

Thermo-mechanical sizing and stress-induced birefringence analysis for the MezzoCielo assembly

Silvio Di Rosa,[a,b,*] Roberto Ragazzoni,[a,b] Marco Dima,[a] Luigi Lessio,[a] Carmelo Arcidiacono,[a] Demetrio Magrin,[a] Jacopo Farinato,[a] and Simone Zaggia[a]

[a]Italian National Institute for Astrophysics, Padua, Italy
[b]University of Padua, Department of Physics and Astronomy, Padua, Italy

ABSTRACT. MezzoCielo telescope aims to be a revolutionary optical instrument, designed to exhibit a field of view of around 10^4 square degrees. As such, it will be able to carry out whole-sky patrolling, which could be exploited, for instance, to track space debris or localize transient phenomena. From an optical stand-point, the telescope is a monocentric lens, composed by an outer glass shell enclosing an inner cavity filled with optical fluid (having proper refractive index for light convergence). From a mechanical point of view, instead, given the limitations related to manufacture large glass elements having high performance, the adoption of a segmented structure, presenting, for example, a platonic solid-like shape, is required. In this paper, the main aspects concerning the sizing of such frame (chosen to be a dodecahedral one) and the thermo-mechanical analysis of the lenses support system assembly, both analytical and numerical, will be presented. In particular, it will be shown how the lenses will be able to operate with little temperature difference across their volume independently from the surrounding conditions and the way in which the telescope can withstand external low temperatures without manifesting high thermal stresses, while maintaining, at the same time, constant focal length. Subsequently, a birefringence investigation, carried out to select the more appropriate lens shape, will be described. From our analysis, pentagonal-shape lenses turn out to be the most suitable ones for the MezzoCielo application.

 [DOI: 10.1117/1.JATIS.10.4.044008]

Keywords: large telescopes; optical fluids; thermo-mechanical sizing; birefringence

Paper 24083G received Jun. 8, 2024; revised Sep. 25, 2024; accepted Oct. 14, 2024; published Nov. 5, 2024.

1 Introduction

MezzoCielo represents a revolutionary concept of global field of view (FoV) optical instruments: it aims to simultaneously survey the whole sky observable from a single site on Earth, exhibiting, at the same time, a relatively large equivalent aperture. Unlike devices devoted to a similar goal, MezzoCielo employs 1-m aperture lenses to achieve a high equivalent collecting surface while maintaining a relatively small size.

The underlying optical design of the telescope is that of a refractive monocentric device, conceived on the idea of a central spherical lens focusing light upon a concentric focal surface on which several cameras, equipped with field lenses and CMOS detectors, are placed. This design is optically effective because it allows increasing the system image quality by reducing to zero all

*Address all correspondence to Silvio Di Rosa, silvio.dirosa@inaf.it

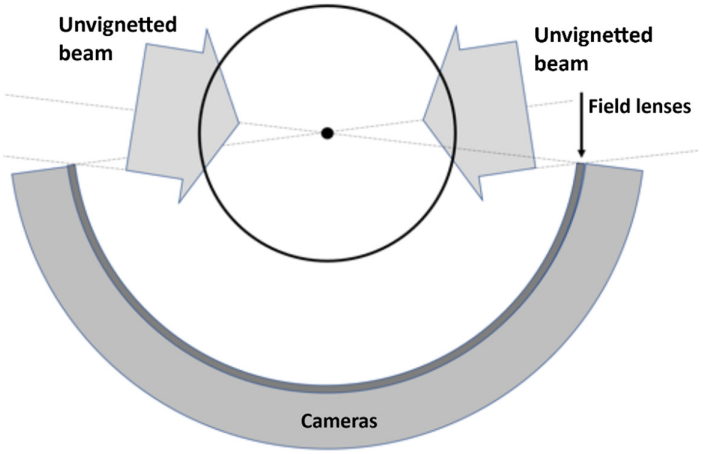

Fig. 1 Example of the MezzoCielo system optical layout, considering limited airmass elevations, such as 15 or 30 deg above the horizon.

the Seidel aberrations, except the spherical one. In addition, the latter is made constant along each of the lines of sight by projecting a virtual stop at the center of the monocentric lens, making in this way the illumination uniform across the entire FoV.[1] A schematic depiction of the MezzoCielo system cross-section is illustrated in Fig. 1.

As stated in Ref. 1, refractive monocentric devices employing bulk glass spherical lens are known, but usually, they are characterized by extremely small apertures. Indeed, realizing a glass sphere having aperture of at least 1 m is not an easy task, particularly in the context of achieving an optical instrument characterized by sufficiently high performance to be employed for scientific purposes. Therefore, two improvements have been hypothesized to solve the technological difficulties and simplify the design:

1. Realizing a hollow sphere with a relatively thin outer glass shell. In this way, it is possible to reduce the overall mass and avoid the critical issues related to the glass substrate inhomogeneities. To make the telescope actually convergent with high focal ratio (greater than 3), the filling of the inner volume of the sphere with proper optical fluid is though required;
2. Dividing the spherical shell in a certain even number of identical meniscus lenses, specularly placed with respect to a plane passing through the center of the sphere, supported one by one. From a mechanical stand-point, this is useful to avoid the realization of a single large glass shell and to provide the proper support, reducing the overall stresses and strains.

Regarding the first point, reducing the amount of glass bulk, generating a two refractive index central system composed by an outer shell of glass, encompassing a inner cavity filled with liquid, is a viable solution for large size systems from a mechanical stand-point.[1] However, such solution is also favorable in terms of optical performance: a large sphere of glass would exhibit a significant spherical aberration, which could be lowered employing, as bulk substrate, an optical material with index slightly smaller than the glass one. Such material should be characterized, in addition to a low refractive index, also by a high-transparency in the visible range (in which MezzoCielo operates), thermal and chemical stability and no toxicity, to give some examples.

In Ref. 2, all the details about the selection and the characterization of the optical fluids are reported. Here, the main results related to the most promising one, the commercially known FC-72, are summarized in Table 1.

Regarding the second point, instead, the lenses have to be supported by a frame which could be circumscribed by a sphere, assuring that the glass elements are equal to each other and arranged in such a manner that the light beam, entering the telescope through one of the lenses, can exit at least through a specular/symmetrical one. Such characteristics suggest the employment, among the possible ones, of a platonic solid configuration, in which the lenses represent

Table 1 FC-72 main properties at $T = 20°C$.

Fluid type	Perfluorohexane, C_6F_{14}
Density	1670 kg m^{-3}
Specific heat	1100 J kg^{-1} K^{-1}
Refractive index n_2 [$\lambda = 580.7$ nm]	1.2512
dn_2/dT [$\lambda = 580.7$ nm]	$-2.961 \cdot 10^{-4}$ K^{-1}
Absorption coefficient [$\lambda = 543$ nm]	$1.616 \cdot 10^{-4}$ m^{-1}

the solid faces and the supporting frame the edges. Indeed, except for the tetrahedron, all the other platonic solids, namely cube, octahedron, dodecahedron, and icosahedron, satisfy the abovementioned requirements. Note that other geometries are eligible for the MezzoCielo application, such as the fullerene one, but that provided by the platonic solids is characterized by the required regularity and design simplicity.

Now, it is crucial to select the most suitable shape to maximize the collecting area, minimizing the overall size. Given a lens of diameter d, the equivalent collecting surface for the several platonic solids presents size, D_{eq}, given by

$$D_{\text{eq}} \propto d\sqrt{\frac{N}{2}}, \tag{1}$$

where N is the solid faces number. The greater the number of faces, the higher the equivalent collecting surface. It is therefore chosen to select the dodecahedral structure and the icosahedral one, with 12 and 20 faces, respectively. For such solids, precise geometric formulas relate the diameter of the circumference inscribed in the single face d with the diameter of the sphere circumscribed to the solid D

$$\begin{aligned} D_D &= \frac{\sqrt{3}(1+\sqrt{5})}{2} tg\left(\frac{\pi}{5}\right) d \approx 2.04d \\ D_I &= \frac{\sqrt{3(10+2\sqrt{5})}}{2} d \approx 3.29d, \end{aligned} \tag{2}$$

where the subscripts D and I indicate dodecahedron and icosahedron, respectively. The equivalent collecting area is also dependent upon the fluid absorption. From the Lambert-Beer law, expressing the transmissibility of a mean having absorption coefficient K and length L,[2] the actual equivalent collection size, neglecting the glass opacity, turns out to be around

$$D_{\text{eq},a} \propto d\sqrt{\frac{N}{2}}(1 - KL). \tag{3}$$

Setting $L = D$ for simplicity and considering the filling of the sphere with FC-72, the ratio $D_{\text{eq},a}/D$ for a dodecahedron and a icosahedron having 1 m aperture faces is 1.2 and 0.91, respectively. For the dodecahedron, the equivalent size is greater than the telescope physical one: with 1-m diameter lenses, the structure would have a size of around 2 m, with 2.5 m of equivalent aperture. A dodecahedral structure is hence selected for the MezzoCielo application. An overall (likely, but not unique) representation of the MezzoCielo assembly is shown in Fig. 2.

In Fig. 2, the monocentric dodecahedral structure is easily recognizable, as well as the pentagonal shape of the lenses, the supporting spider and the focal surface completely filled with cameras. Other configurations are clearly possible.

In the next sections, the main aspects concerning the thermo-mechanical sizing of the MezzoCielo structure and its optical components will be described: temperature and gravitational loads are deemed critical parameters in terms of telescope performance. The facility altitude above the sea level, namely the atmospheric pressure, has, instead, a negligible impact upon the telescope from a mechanical stand-point: according to Pascal's law, the variation of external

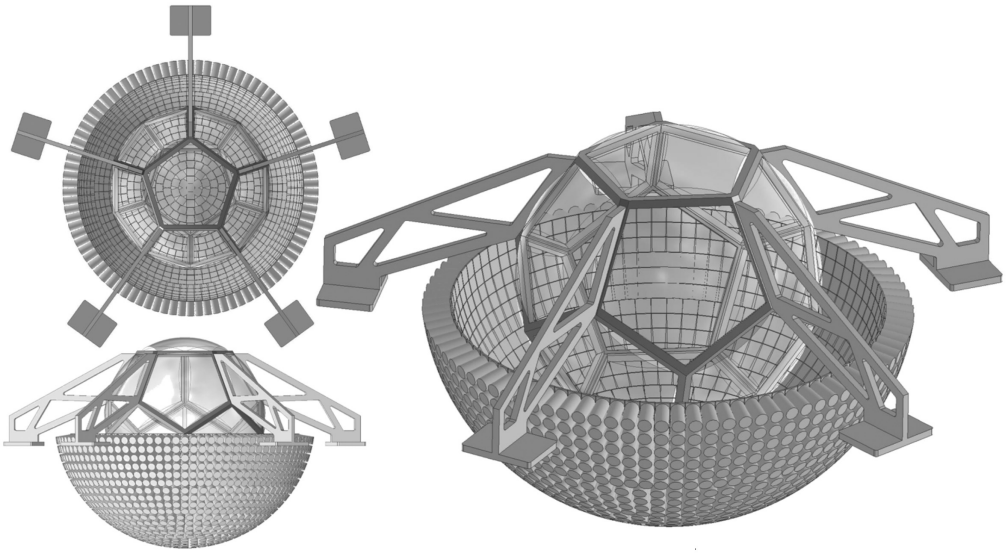

Fig. 2 Visual depiction of a possible layout for MezzoCielo.

pressure around a sphere filled with fluid produces an identical change of the inner pressure (admitting a certain deformability of the shell) and the two effects tend to compensate each other, maintaining unchanged the spherical shape. The analysis presented in this work take into account atmospheric pressure at sea level; however, once the facility site will be selected, a proper investigation should be conducted.

2 Thermo-Mechanical Sizing

For the dodecahedral configuration described in Sec. 1, previous studies[3] have analytically shown that, to achieve a maximum glass deflection (with respect to the reference sphere) not greater than 20 μm, the circular simply supported lens of the assembly, made of BK7, analyzed under the hypothesis of thin plate theory,[4] must present a thickness of at least 120 mm for a 2000-mm diameter sphere. Subsequent finite element analysis (FEA) has actually demonstrated that, for such geometry, load and constraint conditions, the maximum displacement at the lens center is around 10 μm: indeed, the analytical estimation slightly oversizes stresses and strains because the thin plate theory does not consider the actual geometry of the meniscus lens, nor stresses and strains along the axis normal to the lens plane. Moreover, as the outcome of the study performed in Ref. 3, it has been verified that the glass exhibits a linear elastic behavior in the context of the amount of stresses and deformations to which it is subjected. These results, in particular, have been obtained for the lowermost lens of the telescope, located at the bottom of the structure and, as such, subjected to the highest hydrostatic loads. In addition, given the axial symmetric nature of the loads, such a lens deflects in a spherical way, with equal meridional and sagittal radius of curvature.

Given these premises, it is chosen to consider, as the sizing starting point, a dodecahedron inscribed in a 1120-mm radius sphere, comprising 12 identical meniscus BK7 lenses 120-mm thick with clear aperture of 1000 mm each, enclosing a 1000-mm radius sphere filled with FC-72 fluid. A representation of such geometry is sketched in Fig. 3.

In Fig. 3, R_1 represents the radius of the sphere circumscribed to the dodecahedral structure, R_2 the sphere radius containing the fluid, and n_1 and n_2 the glass and fluid refractive index, respectively. The lenses are placed upon the twelve pentagonal faces of the solid, comprised between the two spheres of radius R_1 and R_2. A more accurate representation of the lenses themselves is given in Fig. 4.

Because we are dealing with a dodecahedron, the lenses could have either a pentagonal shape or a circular one. In both cases, the supporting frame must occupy the edges of the pentagonal faces. In this work, the thermo-mechanical behavior of both configurations has been investigated.

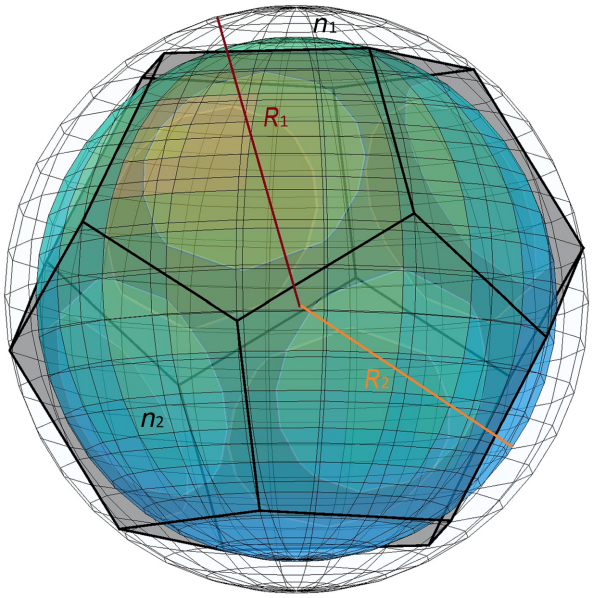

Fig. 3 Schematic representation of the telescope dodecahedral structure. The lenses are not depicted, but they occupy the 12 faces of the solid and are limited by the two sphere of radius R_1 and R_2.

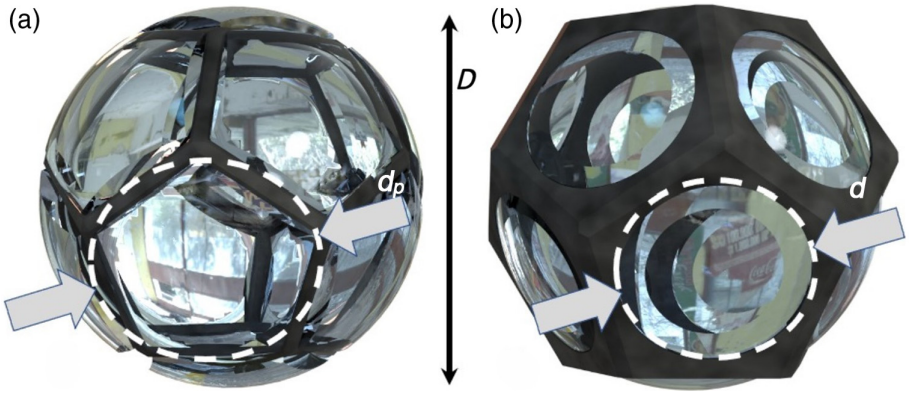

Fig. 4 Realistic representation of the telescope assembly. Because the instrument is, geometrically, a dodecahedron, the lenses could be either pentagonal or circular in shape. The pentagon outer diameter d_p and surface are 24% and 16%, respectively, greater than the circle ones: (a) pentagonal shape lenses and (b) circular shape lenses.

2.1 Radius of Curvature Change Due to Gravitational Loads

To mitigate the geometrical aberrations coming from the lens deformations under the gravitational loads, it is necessary to know the amount of displacement the lenses are subjected to in terms of radius of curvature. To not being limited by the thin plate approximation and given the complex nature of the problem in terms of geometry and loads, it has been chosen to perform finite element analysis for all the lenses of the assembly to estimate stresses, strains, and displacements, relying to analytical calculations only to compute the radius of curvature change.

The telescope will have a face pointing at the local zenith and, therefore, one toward the nadir. Hence, it is possible to recognize an uppermost lens and a lowermost one. In terms of thermo-mechanical behavior, other two lens typologies are significant: the lateral low glass elements (five lenses), adjacent to the lowermost lens and pointing 26.55 deg below the horizon, and the lateral high ones (five lenses), adjacent to the uppermost one and pointing 26.55 deg above the horizon. Each kind of glass element, given its placement within the dodecahedral structure, is characterized by a certain type of load:

1. The lowermost lens is subjected to a hydrostatic load given by the weight of a fluid column of length $2R_2$. The related pressure, the highest among those beared by the lenses, is distributed in an axial-symmetrical way. The lens weight is added to the hydrostatic force, having the same direction, and the lens radius of curvature tends to decrease;
2. Each of the five lateral lenses placed in the dodecahedron lower hemisphere forms with the horizontal plane (where lies the lowermost lens); the dihedral angle of 116.55 deg, namely they are inclined of 26.55 deg with respect to the gravity vector. As such, they are subjected to their own weight, with the gravity vector rotated of 63.45 deg (toward the lowermost lens) with respect to the normal to the lens plane, and to the hydrostatic pressure, acting normally to the plane of the lens and linearly variable along the lens diameter. For these lenses, the hydrostatic force and the lens weight component normal to the lens plane present the same direction and the radius of curvature hence reduces. Given the not axial symmetric loads, the radius of curvature in the meridional plane of the lens will be different from that in the sagittal one, producing a cylindrical deformation (at least in a first-order approximation);
3. For the five lateral lenses located in the higher hemisphere, the same considerations described above for the lower hemisphere lenses apply, but hydrostatic force and lens weight exhibit opposite directions and they tend to compensate each other;
4. The uppermost lens is subjected to its own weight, which tends to increase the radius of curvature. The load is again axial symmetric and the deformation follows a spherical pattern.

In Fig. 5, the displacements along the direction parallel to the lens optical axis (Z axis) are depicted for all the optical elements of the assembly, considered with both pentagonal and circular shape (the lens lies in the X–Y plane). Such displacements are computed with respect to an unloaded lens, characterized by an ideal meniscus shape geometry with outer and inner radius, respectively, of $R_1 = 1120$ mm and $R_2 = 1000$ mm. The lenses are simply supported along the edges.

In the same Fig. 5, the positive sign denotes outward displacements, whereas the negative one inward displacements, namely toward the sphere center. The numerical analysis described in these figures (and in the following as well) have been carried out using the *AutoCad* tool *Fusion360*.

In Tables 2 and 3, instead, the lenses maximum displacement and the corresponding radius changes in the meridional and sagittal plane with respect to the nominal value of $R_1 = 1120$ mm are reported for circular and pentagonal lenses, respectively. These results have been achieved for lenses simply supported along the edges. Moreover, both shapes have been defined on the basis of considerations reported in Sec. 2.3.

The plus sign in the second column of Tables 2 and 3 indicates outward displacement, while that in the third and fourth ones, a radius increase.

In summary, Fig. 5 and Tables 2 and 3 suggest that the pentagonal lens, given the same boundary conditions, exhibits lesser deformations with respect to the circular one. This could be due to the fact that the supports along the long edges of the pentagonal shape are closer together than those for the circular one and so allow smaller deflections in one meridian. Now, the radius of curvature tolerances for precise optics can be as small as 0.01% of the radius itself, namely, in this case, around 100 μm. Observing the expected variation of the radius of curvature in Tables 2 and 3, it can be noted that such deviations are slightly lesser than the construction tolerances: this suggests that the gravitational loads do not produce an appreciable modification of the lens shape, that is, they do not substantially affect the telescope sphericity.

2.2 Thermo-Mechanical Design

The focal length of a monocentric lens composed by an outer shell and an inner cavity of different materials, having refractive indices n_1 and n_2, respectively, can be written as

$$f = \frac{R_1 R_2 n_1 n_2}{2(n_1 - 1)R_2 n_2 + 2(n_2 - n_1)R_1}. \tag{4}$$

At 580.7 nm, the fluid refractive index n_2 is given in Table 1, whereas the Schott datasheet[5] provides the value of $n_1 = 1.5168$ for the BK7 glass. From this parameter, it is

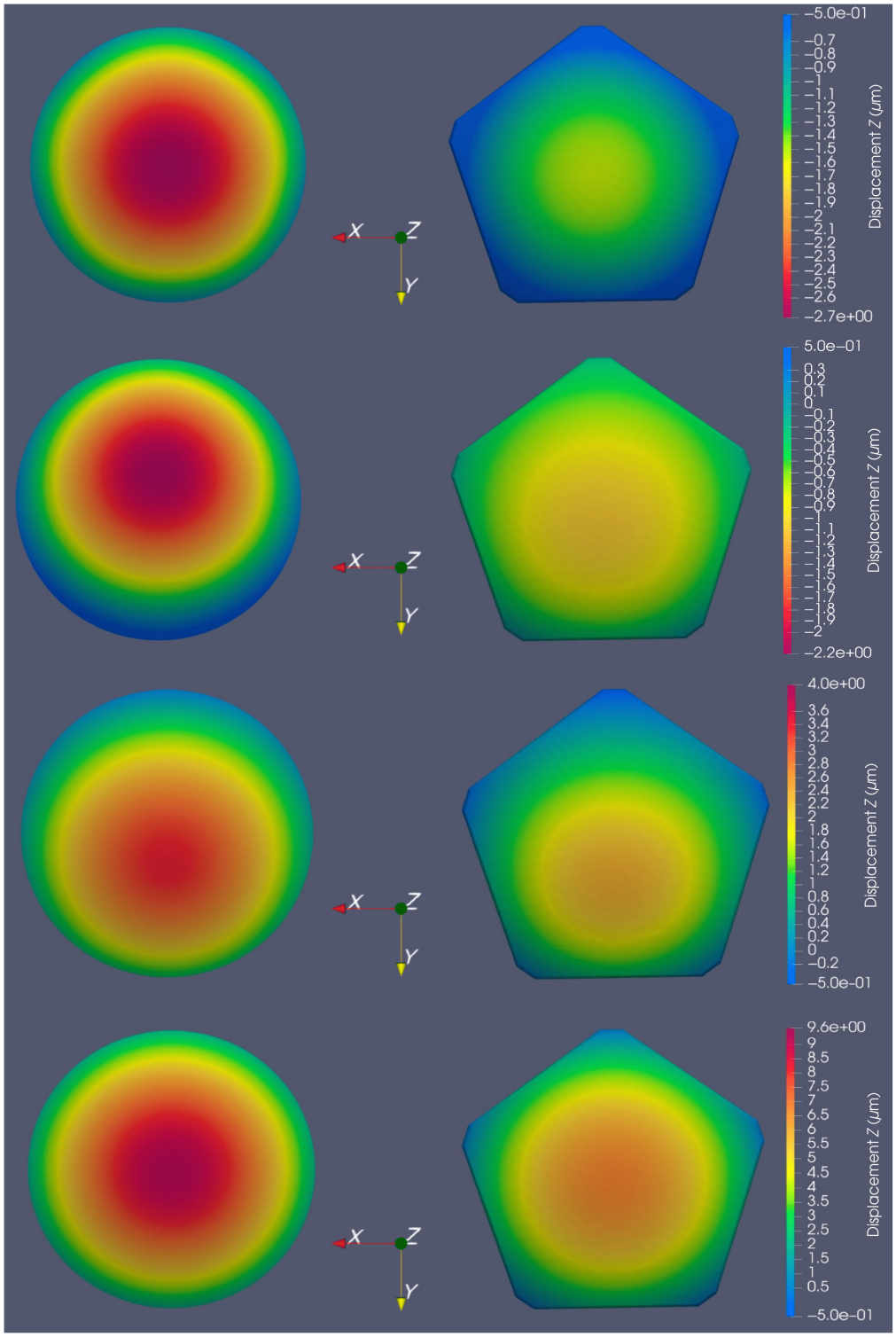

(a) (b)

Fig. 5 Z displacements of the MezzoCielo lenses subjected to gravitational loads. From the top: uppermost, upper hemisphere, lower hemisphere, and lowermost lenses. (a) Circular lenses and (b) pentagonal lenses.

immediate to obtain a focal length of 3044.4 mm. Now, considering for the telescope a filling factor $\eta = h/R_1 = 0.5$, with h height of the marginal ray with respect to the lens optical axis, the depth of focus (DoF) of the monocentric device can be computed from the optics rules:

Table 2 Maximum displacements and radius changes for circular lenses with only gravitational loads acting.

	Max displacement (μm)	ΔR_1 – meridional (μm)	ΔR_1 – sagittal (μm)
Lowermost lens	+9.6	−85	−85
Lateral low lenses	+3.9	−26	−32
Lateral high lenses	−2.2	+9	+12
Uppermost lens	−2.7	+8	+8

Table 3 Maximum displacements and radius changes for pentagonal lenses with only gravitational loads acting.

	Max displacement (μm)	ΔR_1 – meridional (μm)	ΔR_1 – sagittal (μm)
Lowermost lens	+7.1	−59	−59
Lateral low lenses	+2.4	−18	−21
Lateral high lenses	−1.1	+8	+9
Uppermost lens	−1.5	+8	+8

$$\mathrm{DoF} = 2(F/\#)c = \frac{R_1^2}{64f}, \tag{5}$$

being c the diameter of the least confusion circle and $F/\#$ the telescope F-number.

The uncertainty associated with the focal length, Δf can, instead, be computed from the uncertainties propagation:

$$\Delta f = \sqrt{\left(\frac{df}{dR_1}\Delta R_1\right)^2 + \left(\frac{df}{dR_2}\Delta R_2\right)^2 + \left(\frac{df}{dn_1}\Delta n_1\right)^2 + \left(\frac{df}{dn_2}\Delta n_2\right)^2}. \tag{6}$$

Setting $\Delta f = DoF/2$, the required tolerance associated with the radius of curvature is around 400 μm, that is 0.035% of R_1. Such result has been achieved considering for the BK7 refractive index n_1 the tolerance value of 0.0002 as prescribed by Schott, while for the FC-72 refractive index, measurements reported in Ref. 3 suggest a tolerance value of 0.0004 for n_2. Regarding the sensitivity coefficients, instead, their values were computed from Eq. (4) at room temperature (20°C). Such coefficients are listed in Table 4.

In summary, employing BK7 lenses with high-quality optical properties and FC-72 as optical fluid, the focal length uncertainty is comparable with the depth of focus. As a requirement, we may impose that the thermo-mechanical loads do not affect the focal length more than the desired tolerance of DoF/2. As seen in Sec. 2.1, the gravitational loads do not alter significantly the radius of curvature, because they produce a radius change lesser than 100 μm. A crucial point

Table 4 Sensitivity coefficients of the MezzoCielo focal length at $T_0 = 20$°C.

	Sensitivity coefficient value
df/dR_1	5.035
df/dR_2	−0.278
df/dn_1 [mm]	863.241
df/dn_2 [mm]	−11841.271

is then the modification of R_1, R_2, n_1, and n_2 with temperature. A good design must, hence, take into account this aspect.

Because the telescope will probably be installed in a mountain location on the Alps in Italy, it is possible to hypothesize for MezzoCielo a temperature range of $[-5, +20]$°C, based on the average temperatures registered at the Mount Ekar observation station in Asiago,[6] where is located the largest telescope on the Italian territory. The temperature variation in this thermal range must not produce an alteration of the main parameters greater than the uncertainty coming from manufacturing and measurements. The values of the sensitivity coefficients df/dR_1, df/dR_2, df/dn_1, and df/dn_2, reported in Table 4, evaluated at the room temperature $T_0 = 20$°C, clearly shows that the focal length is primarily influenced by the refractive indices.

Regarding the thermal variation of the BK7 refractive index, the latter can be estimated using the formulas provided by Schott in Ref. 7. From simple calculations, it has been verified that the absolute variation of n_1 in the thermal interval taken into account is one order of magnitude less than the manufacturing tolerances guaranteed by Schott. The related focal length change is around 35 μm, around two orders of magnitude lesser than the uncertainty Δf.

For the liquid refractive index, instead, in Ref. 2, it has been shown that the fluid expected thermal variation follows a cubic trend in the temperature range $[-5, +20]$°C. Therefore, it is easy to verify that to obtain a maximum index variation of 0.0004, the fluid temperature must not deviate more than 1°C from the nominal temperature T_0. This means that during the observations, the liquid temperature has to be kept constant between 19°C and 20°C employing a re-circulation system. Such a solution reveals useful because, in this way, it could be possible to exploit the high thermal capacity of the liquid mass to warm the entire instrument, avoiding excessive temperature difference between its several components.

As a case study, we can suppose that the telescope is continuously employed for 8 h at the (constant) external temperature of $T_e = -5$°C. We are interested in estimating the temperature drop the lenses are subjected to.

Considering a constant (room) temperature for the fluid, it is possible to write a thermal balance equation for the entire telescope:

$$(Mc_p)_g \frac{dT}{dt} = \frac{T_0 - T}{R_{\text{th},g}} - h_{\text{conv}} \pi D^2 (T - T_e). \tag{7}$$

In Eq. (7), M represents the glass shell mass, c_p the BK7-specific heat, $R_{\text{th},g}$ the thermal resistance of the spherical glass shell, t time, and D the telescope diameter, while T represents the telescope outer surface temperature. The convective coefficient h_{conv} is, instead, computed employing the heat transfer theory applied to a sphere immersed in quiet air, therefore in natural convection regime. For a sphere of radius $R_1 = 1120$ mm and air temperature $T_e = -5$°C, it is estimated a value of 2.81 $\text{W m}^{-2}\,\text{K}^{-1}$ for the convective coefficient.

Solving Eq. (7), the time law ruling the variation of T is obtained:

$$T(t) = (T_0 - T_p) \exp\left(-\frac{t}{\tau}\right) + T_p, \tag{8}$$

being τ the instrument thermal constant and T_p the steady-state temperature. Because $\tau \approx 20\,000$ s and $T_p \approx 14.5$°C, after 8 h, the lenses outer surface would reach a temperature of around 16°C, namely a temperature difference of 4°C would be established across the glass shell. The radius decrease can be approximated by

$$\Delta R_1 = R_1 CTE_g \Delta T, \tag{9}$$

where CTE_g is the BK7 coefficient of thermal expansion. Such decrease is about -32 μm.

Now, because the lenses cannot move along their edges, it is possible to hypothesize that the variation computed in Eq. (9) concerns mainly the glass central portion. Therefore, such value must be added (with its sign) to those reported in Tables 2 and 3 to estimate the central displacements. The latter are reported in Tables 5 and 6.

Even considering the thermal influence, the expected radius change remains lesser than the required tolerance. In such conditions, the fluid temperature variation can be computed from

Table 5 Maximum displacements and radius changes for circular lenses with thermal and gravitational loads acting.

	Max displacement (μm)	ΔR_1 – meridional (μm)	ΔR_1 – sagittal (μm)
Lowermost lens	−22.4	−187	−187
Lateral low lenses	−28.1	−238	−251
Lateral high lenses	−34.2	−289	−344
Uppermost lens	−34.7	−295	−295

Table 6 Maximum displacements and radius changes for pentagonal lenses with thermal and gravitational loads acting.

	Max displacement (μm)	ΔR_1 – meridional (μm)	ΔR_1 – sagittal (μm)
Lowermost lens	−24.9	−212	−212
Lateral low lenses	−29.6	−252	−266
Lateral high lenses	−33.1	−281	−334
Uppermost lens	−33.5	−285	−285

$$(Mc_p)_f \frac{dT_f}{dt} = \left(\frac{1}{R_{\text{th},g}} - h_{\text{conv}}\pi D^2\right)(T_f - T_e), \tag{10}$$

where the subscript f indicates fluid properties. Note that the fluid temperature T_f is supposed uniform across the liquid volume. Solving Eq. (10), it is achieved that the liquid temperature decreases by 1°C after around 2.5 h. Therefore, the warming system associated with the telescope has to be activated up to three times during a night of observations.

Up to this point, the telescope thermal balance has been written considering quiet air around the sphere, namely the natural convection regime has been assumed as working hypothesis. If one desires to consider wind effects, in Eq. (7), the convective coefficient h_{conv} has to be substitute with h_w given by

$$\text{Re} = \frac{VD}{\nu} \quad \text{Nu} = 2 + (1.6\,\text{Re}^{1/3} + 0.6\,\text{Re}^{1/2} + 0.005\,\text{Re}^{0.8})\text{Pr}^{1/3} \quad h_w = \frac{k\text{Nu}}{D}, \tag{11}$$

where V is the wind velocity; ν, Pr, and k represent the cinematic viscosity, Prandtl number, and conductivity coefficient of air at $T_e = -5$°C, respectively, whereas Re and Nu are the Reynolds and the Nusselt numbers characterizing this forced convection situation. Considering the average value of wind speed registered in the Asiago site in winter, around 5 m/s, the convective coefficient results to be $h_w = 9.18\ \text{W m}^{-2}\,\text{K}^{-1}$ and the glass shell exhibits a temperature drop of 4°C after around 2 h.

2.3 Frame Sizing

We will now focus upon the sizing of the frame supporting the lenses and on the coupling between such elements.

The starting point is the frame material choice. The lattice has to provide the required rigidity to reduce the lenses displacements, without reaching the yielding strength limit; moreover, its material has to exhibit a coefficient of thermal expansion (CTE) similar to the BK7 one to minimize thermal stresses, has to be compatible with fluorine fluids, affordable and feasible in large quantities. Such characteristics lead to the choice of metallic materials. Among them, it has been selected Kovar, a iron-nickel-cobalt alloy, which exhibits the same elasticity, strength, and possibility of mass production of steel, but with a CTE significantly lesser.

The sizing of the Kovar frame is based on the following considerations, which represent constraints and requirements:

1. The frame will occupy the edges of a dodecahedron inscribed in a 1120-mm radius sphere. Hence, pentagonal faces have to be realized with edges of 799.281 mm;
2. Because the frame has to support the lenses, the lattice is conceived as a sequence of L-shape beams arranged along the edges of the platonic solid. Moreover, to assure a proper interface between the pentagonal support of the single lens, each of the L-shape beam has to exhibit, along the edge direction, an inclination of 26.55 deg toward the center of the solid itself;
3. The flanges of the beams are in contact with the fluid. To minimize their deflections, allowing at the same time a good interface between lenses and frame, it is chosen to consider 20-mm long, 10-mm thick flanges. From construction science, such dimensions should ensure a flange deflection less than 2 μm (it should be noticed that such value was obtained considering the flange itself clamped at one end—that in contact with the pentagonal frame—and subjected to the lens weight, modeled as a distributed load along the flange free edge). The 1000-mm clear aperture of the lenses is therefore surrounded by the frame flanges;
4. The height of the L-shape beam is constrained by the overall geometry. To allow a clear aperture of 1000 mm and to realize a dodecahedral lattice fitting exactly within a 1120-mm radius sphere, the frame L-beams should be no more than 45 mm high, with webs of 35 mm;
5. To improve the quality of the coupling frame-lenses in terms of displacements, a 10-deg taper angle is foreseen.

Strictly speaking, such considerations apply for a frame supporting lenses of pentagonal shape. For circular lenses, the frame cannot be simply seen as an assembly of L-beams and the area it covers is around 2.3 times greater than that requested for pentagonal shape lenses.

Regarding the lens geometry, the outer radius has to be 1120 mm, with thickness of 120 mm and 1000 mm clear aperture. The contact with the frame will take place along the entire length of the frame webs and flanges. Given the need for this type of coupling, it is possible to estimate that the pentagonal shape lens, occupying around 90% of the dodecahedral face surface, exhibits a collecting area around 1.17 times greater than the circular one (which occupies 77% of the entire face). For both lenses, sharp edges should be smoothed out creating chambers: it is immediate to observe that such operation is much more critical for the pentagonal lens, which requires, in addition to those of the circular lens, also the beveling of all the five sharp corners to avoid stress concentrations. The size of the beveling has been firstly chosen arbitrarily, and then, after several finite element simulations, it has been selected the one assuring minimum stress. The lenses lateral sides exhibit a 10-deg taper angle. The front and rear views of the single lens assembly are depicted in Fig. 6 for both pentagonal and circular glass elements.

In terms of thermal design, it is desirable that the metallic frame temperature exhibits the same variation law of the glass shell. The values of τ and T_p in Eq. (7) have hence been used to estimate the required frame thermal resistance. After some calculations, we found that for the frame to show a thermal gradient similar to the glass one, it has to be covered with an insulating material having thermal conductivity of around 0.025 $\mathrm{W\,m^{-1}\,K^{-1}}$: a polyurethane layer 7.5-mm thick for the pentagonal shape lens and 5-mm thick for the circular one should assure the required thermal balance. The equivalent thermal resistance given by the frame and lenses ones, arranged parallel to each other, is consistent with the glass shell total resistance employed in Eq. (7).

Finally, regarding the coupling between lenses and frame, it is chosen to employ adhesive bonding. Indeed, adhesives distribute stresses more uniformly than mechanical fasteners, are more flexible, lighter in weight, lower in cost, and easier to assemble than those made by mechanical methods.[8] For the side bonding, the one bearing the most load, the two components epoxies Milbond is employed as structural adhesive. The axial joint, instead, has to provide primarily the watertightness of the system; therefore, it must not chemically react with the fluid, along with a reasonable degree of rigidity and strength. Even though the most employed sealants are the silicone based adhesives, the latter are not suitable for the MezzoCielo application due to their low joint strength. A suitable alternative could be then represented by the Scotch-Weld Epoxy Adhesive 2214 Regular, a one part epoxy produced by 3M Company, which combines high rigidity, strength, and sealing properties.

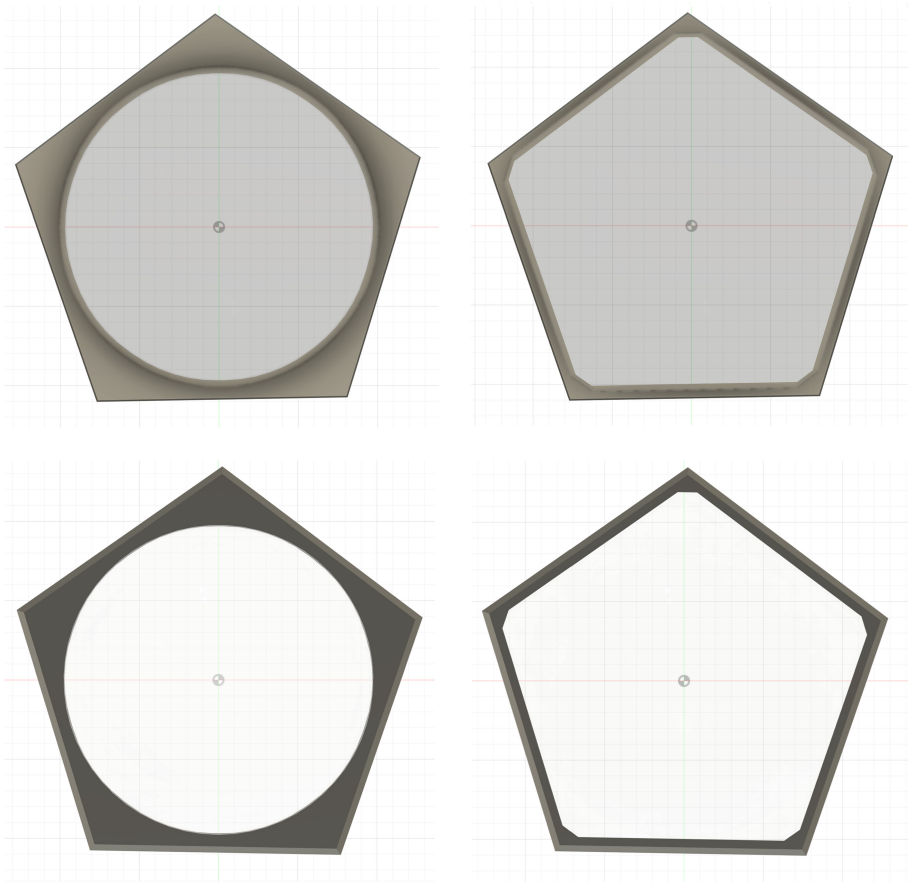

Fig. 6 Front (top) and rear (bottom) view of the MezzoCielo lens assembly: (a) circular lenses and (b) pentagonal lenses.

A first sizing of the adhesive layers could be done in terms of athermalization. Indeed, as suggested in Ref. 8, if the bonding layer has a particular thickness, the assembly will, to a first-order approximation, be athermal in the radial and axial direction. This minimizes stresses build-up within the opto-mechanical components which are caused by differential expansion or contraction of the lens, mounting and adhesive under temperature changes. This thickness can be computed with

$$t_a = l\frac{(1-\nu_a)(\mathrm{CTE}_m - \mathrm{CTE}_g)}{\mathrm{CTE}_a - \mathrm{CTE}_m - \nu_a(\mathrm{CTE}_g - \mathrm{CTE}_a)}. \tag{12}$$

In Eq. (12), ν_a is the adhesive Poisson's ratio and the subscripts a, m, and g refer to adhesive, metal, and glass, respectively. With Eq. (12), we can compute the structural adhesive thickness substituting to the length l the lens radius $d/2$ and the sealant thickness if $l = t$, being t the lens thickness. Strictly speaking, Eq. (12) applies to annular adhesive layer placed radially along the lens circumference: the employment of this formula to size the axially located layer of sealant in terms of athermalization should be considered a first-order approximation to be verified through the numerical simulations.

In Table 7, the materials taken into account for the several components of the telescope assembly are listed along with their main properties, namely Young's module E, bending, yield and shear strength for glass, metal, and adhesives, respectively, thermal conductivity k and CTE. Such properties can been retrieved in Refs. 5, 8, and 9. In particular, the bending strength of a glass is a complex function of both chemical composition and surface finish. In the context of this work, for BK7, it was chosen to consider one of the lowest values of strength reported by Schott

Table 7 Telescope assembly materials main properties.

	Material	E (MPa)	Strength (MPa)	k ($W\,m^{-1}\,K^{-1}$)	CTE (K^{-1})
Lenses	BK7	82,000	48	1.2	$7.1 \cdot 10^{-6}$
Frame	Kovar	138,000	345	17	$6.5 \cdot 10^{-6}$
Adhesive	Milbond epoxy	592	17.7	1.36	$62 \cdot 10^{-6}$
Sealant	2214 reg. epoxy	5170	20.7	0.4	$49 \cdot 10^{-6}$
Insulating	Polyurethane	/	/	0.025	/

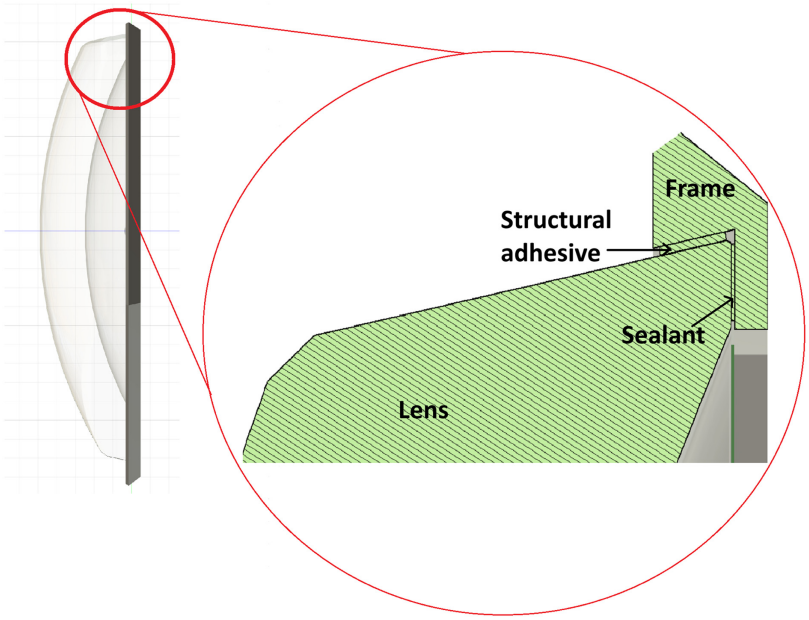

Fig. 7 Side view of the MezzoCielo lens assembly and its main components.

in Ref. 10, namely the 50% probability failure breakage bending strength for glass with "coarse" surface finish.

By virtue of the CTE values in Table 7, we obtain, on the basis of Eq. (12), a thickness of 2 mm for the structural adhesive and 0.5 mm for the sealant. Given the frame dimensions and the forces at stake, it is chosen to employ a 20-mm wide structural adhesive layer and a 18-mm wide sealant layer. In this way, almost the entire lens-frame interface surface would be covered with adhesive, except for few millimeters, useful to allow the expansion under the gravitational loads. The side view of the single lens assembly with a zoom detailing the arrangement of lens, frame, structural adhesive, and sealant is reported in Fig. 7.

As defined in geometry, materials, and thermo-mechanical loads, it is now possible to perform finite element analysis of the pentagonal and circular assemblies to verify the analytical results and the actual system feasibility.

3 Results and Discussion

In this section, the main results of the finite element analysis are presented for all the telescope lenses, considered both pentagonal and circular in shape, in terms of temperatures, safety factors, and displacement distribution. The gravitational loads taken into account descend from the mass values reported in Table 8 for all the main components of the MezzoCielo system. In this table, the fluid mass is given by the product between the telescope inner volume, $V_i = (4/3)\pi R_2^3$, and the fluid density, $\rho_f = 1670\ \mathrm{kg/m^3}$; the telescope mass is, instead, computed as the sum of the mass of the 12 lens-frame systems and that of the fluid.

Table 8 Mass of MezzoCielo telescope and its main elements.

	Mass (kg) – pentagonal lenses	Mass (kg) – circular lenses
Lens (BK7)	257	213
Frame (Kovar)	30	85
Fluid (FC-72)	~7000	~7000
Whole telescope	~10,500	~10,600

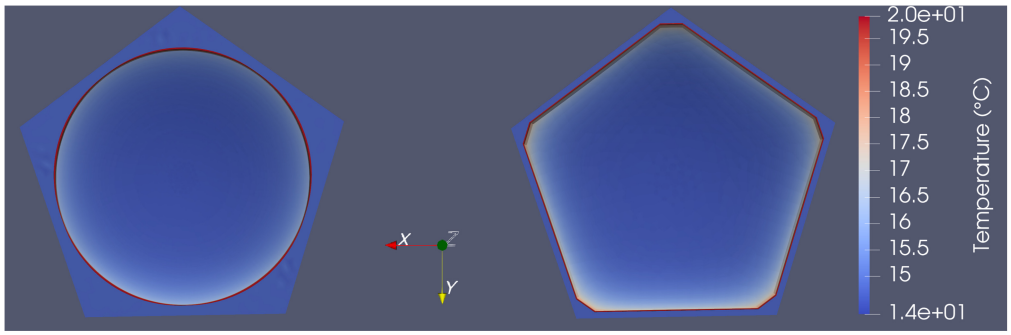

(a) (b)

Fig. 8 Temperature distributions upon the outer surface of the lenses assemblies: (a) circular lens and (b) pentagonal lens.

For a thermal description of the systems under analysis, we can refer to Fig. 8, in which the outer surface of the lenses assemblies is depicted for both pentagonal and circular glass elements.

The results in Fig. 8 have been achieved considering a steady-state situation, characterized by a (constant) outer temperature of −5°C in natural convection regime and assemblies inner surface at the constant temperature of 20°C (not shown in Fig. 8). The numerical results confirm that regardless of the lens shape, the lowest temperature reached by the optical device is around 14°C and, above all, that such temperature is the same for both frame and glass components: the temperature differences are so minimized and stresses and strains as well.

Regarding the safety factors, the latter are computed using the following formula:

$$\mathrm{SF} = \frac{\sigma_{\mathrm{al}}}{\sigma_{\mathrm{max}}}, \tag{13}$$

where σ_{al} represents the ultimate stress the material is allowed to withstand before reaching the yield or the tensile strength limit, while σ_{max} is the maximum stress which occurs in the component as a consequence of the applied loads. The allowable stress is, in turn, computed as the ratio between the material limit strength (reported in the fourth column of Table 7) and a safety coefficient c_s, chosen arbitrarily greater than 1. This coefficient and related allowable stress are reported in Table 9 for the materials taken into account.

Table 9 Safety coefficient and allowable stress for the MezzoCielo materials.

Material	Strength (MPa)	c_s	σ_{al} (MPa)
BK7	48	1.7	28
Kovar	345	1.5	230
Milbond epoxy	17.7	2	9
reg. epoxy	20.7	2	10

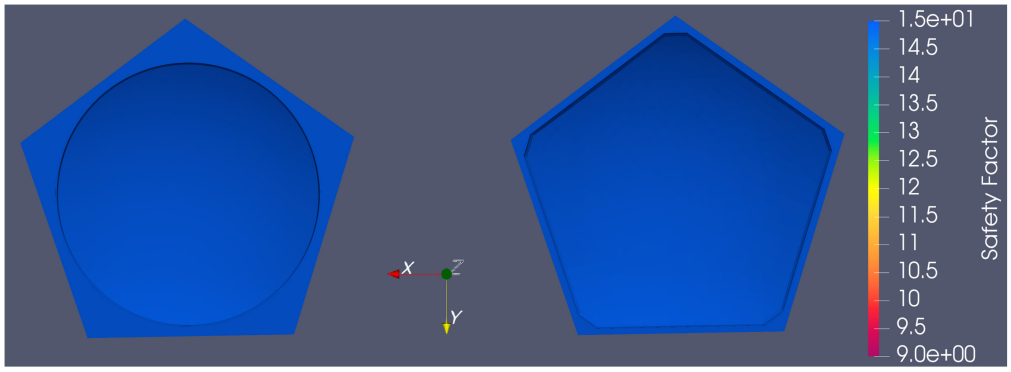

Fig. 9 Safety factors distribution for the lenses assemblies: (a) circular lens and (b) pentagonal lens.

The maximum stress, instead, is computed in terms of Von Mises stress for the metallic frame and maximum principal stress for glass and adhesives. Several simulations have demonstrated that the most critical situation (characterized by the highest stresses, namely the lowest safety factors) occurs when a combination of thermal and gravitational loads is taken into account. In Fig. 9, it is reported the safety factors distribution for the lowermost lens, subjected, in addition to its own weight, to the highest hydrostatic pressure and to the thermal loads descending from the configuration described in Fig. 8. Along the pentagonal frame edges, a fixed constraint (with no displacements and rotations possibility in the X, Y, Z directions) has been applied.

As it can be noticed by observing Fig. 9, the safety factors are higher than 14 for each component of both assemblies: this assures the design robustness and a promising result in the context of the telescope actual realization.

The displacement distribution is, instead, shown in Fig. 10 for all the lenses, both pentagonal and circular in shape. Loads and constraints are those described above for the safety factors simulation: a temperature difference of about 6°C across each assembly, gravitational loads modulated as a function of the assembly inclination with respect to the gravity vector and fixed frame edges are therefore the boundary conditions of the analysis.

In the same Fig. 10, the lens displacements are computed considering the glass elements bonded to the metallic frame, which is not shown; the positive sign denotes outward displacements, the negative one inward displacements, and toward the telescope center.

A comparison between Figs. 5 and 10 clearly shows that the temperature influence is much more pronounced with respect to the gravitational loads one: indeed, the overall displacements reported in Fig. 10 not only present higher absolute values but also for all the lenses, regardless of their location in the telescope assembly, they exhibit an inward shift with approximately the same pattern, namely a spherical one, with maximum values at the center and minimum ones at the edges; the cylindrical deformation, typical of the lateral lenses subjected to the mechanical loads alone, is hence strongly reduced. In addition, Tables 5 and 6 suggest that the analytical results slightly oversize displacements and radius changes as well. Given the same load and constraint conditions, the pentagonal lenses displace less than the circular ones, probably as a consequence of their supports arrangement, which tends to keep unchanged their position and the related deformation.

4 Stress and Birefringence

In this section, the birefringence analysis of the MezzoCielo glass elements is performed: the objective is the quantification of birefringence in terms of refractive index change and phase retardation along the principal stresses directions. The latter quantity, in particular, will be employed to compute the Mueller matrix for each lens, with which it will be possible to characterize the polarization type induced by these relatively large glass elements.

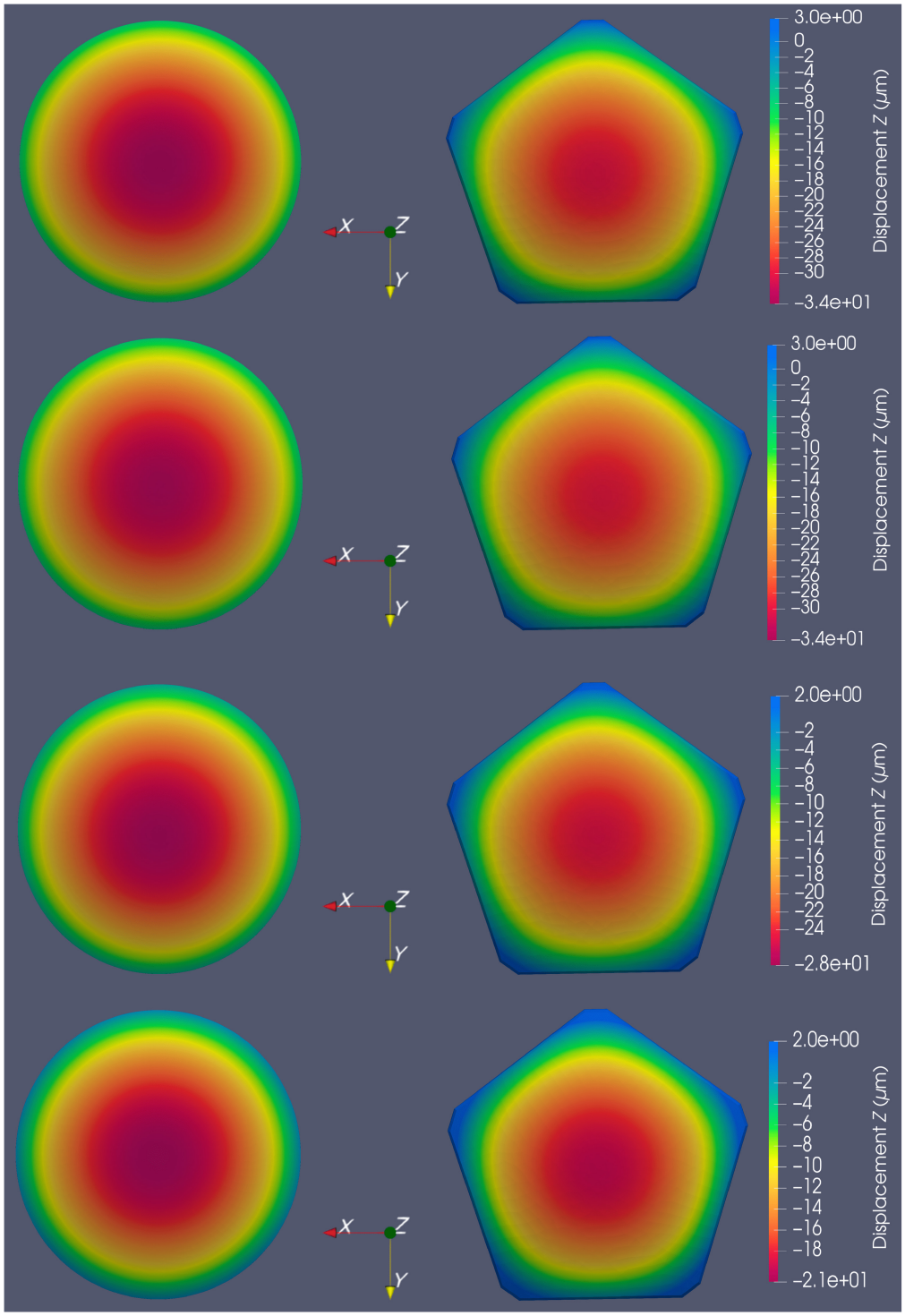

Fig. 10 *Z* displacements of the MezzoCielo lenses subjected to thermal and gravitational loads. From the top: uppermost, upper hemisphere, lower hemisphere, and lowermost lenses. (a) circular lenses and (b) pentagonal lenses.

The birefringence phenomenon happens when the refractive index of a glass, normally isotropic, becomes locally anisotropic due to the presence of stress. This means that, along the directions parallel and perpendicular to that of the stress, a difference in the values of n is established, which, in turn, produces phase retardation and optical path difference proportionally to the stress itself.[11]

The birefringence analysis follows the procedure employed in Ref. 12. Therefore, from the FEA executed in *Fusion360*, the stress tensor for each node of each lens has been estimated

$$\text{StressTensor} = \begin{pmatrix} \sigma_x & \tau_{xy} & \tau_{xz} \\ \tau_{yx} & \sigma_y & \tau_{yz} \\ \tau_{zx} & \tau_{zy} & \sigma_z \end{pmatrix}, \tag{14}$$

where σ and τ represent the normal and shear stresses, respectively, computed in a coordinates system XYZ with the Z axis parallel to the sphere normal and directed outward and the lens lying in the XY plane. For each stress state, one can identify a mutual orthogonal system in which the shear stresses are zero, acting only the normal components of stress. The latter are called principal stresses, and they act along principal directions, normal to the principal planes. In other words, in each point, the stress state can be analyzed only in terms of normal components of stress: because we are dealing with a tri-axial state of stress, we recognize a first, second, and third principal stress, σ_1, σ_2, and σ_3. It can be demonstrated[12] that such quantities are the eigenvalues of the eigenproblem associated to the stress tensor Eq. (14), namely they are the roots of the cubic characteristic equation of the stress tensor

$$\sigma^3 - I_1\sigma^2 + I_2\sigma - I_3 = 0, \tag{15}$$

where I_1, I_2, and I_3 are the principal scalar invariants, functions of the normal, and shear stress components

$$\begin{aligned} I_1 &= \sigma_x + \sigma_y + \sigma_z \\ I_2 &= \sigma_x\sigma_y + \sigma_y\sigma_z + \sigma_x\sigma_z - \tau_{xy}^2 - \tau_{yz}^2 - \tau_{xz}^2 \\ I_3 &= \sigma_x\sigma_y\sigma_z - \sigma_x\tau_{yz}^2 - \sigma_y\tau_{xz}^2 - \sigma_z\tau_{xy}^2 + 2\tau_{xy}\tau_{yz}\tau_{xz}. \end{aligned} \tag{16}$$

The principal directions are, instead, the eigenvectors and can be obtained after having computed the principal stresses.

The stress tensor and corresponding principal stresses and directions have hence been estimated for each lens of the assembly, considering both gravitational and thermal loads acting. In particular, it has been verified that the eigenvector associated to the third principal stress is parallel to the sphere normal (actually, this fact is strictly true for the lenses central portion, the one mostly interested by the light passing, while along the edges and the vertices—for the pentagons—such statement represents an approximation, because the third principal direction can deviate from the sphere normal up to 20 deg). Therefore, at least in the first approximation, we can compute the amount of birefringence as

$$\Delta n = k_g(\sigma_1 - \sigma_2), \tag{17}$$

where σ_1 and σ_2 are the first and second principal stresses whose eigenvectors lie in the plane perpendicular to the sphere normal, while k_g is the glass stress-optical coefficient, function of wavelength, glass type, and temperature. For BK7, at the room temperature of 20°C and in the visible range, $k_g = 2.76 \cdot 10^{-6}$ mm^2/N. When light propagates through a birefringent material with birefringence Δn and thickness t, the corresponding phase retardation δ can be estimated as

$$\delta = \frac{2\pi}{\lambda}(\Delta n)t. \tag{18}$$

In Tables 10 and 11, a summary of the maximum values of principal stresses, refractive index difference, and phase retardation for the circular and pentagonal lenses, computed for glass thickness of 120 mm and $\lambda = 580.7$ nm, is reported. A visual representation of the amount of birefringence and phase retardation is, instead, depicted in Figs. 11 and 12, respectively, for all the lenses of the assembly, both pentagonal and circular in shape.

As we can see from the above figures and tables, birefringence and phase difference increase passing from the lens center to the edges, as a consequence of the fact that the first principal stress values are the highest in the latter regions. The related optical path difference goes from 0 to around $\lambda/2$ passing from the lenses center to the edges. Moreover, the birefringence, proportional

Table 10 Principal stresses, refractive index difference, and phase retardation max values for the circular lenses at $T_e = -5°C$.

Lens type	$\sigma_{1,max}$ (MPa)	$\sigma_{2,max}$ (MPa)	$\sigma_{3,max}$ (MPa)	Δn ($\cdot 10^{-6}$)	δ (rad)
Uppermost	0.99	0.63	0.13	2.2	2.7
Lat. high	1.0	0.65	0.13	2.1	2.5
Lat. low	1.1	0.81	0.25	2.6	3.3
Lowermost	1.1	1.0	0.25	2.6	3.3

Table 11 Principal stresses, refractive index difference, and phase retardation max values for the pentagonal lenses at $T_e = -5°C$.

Lens type	$\sigma_{1,max}$ (MPa)	$\sigma_{2,max}$ (MPa)	$\sigma_{3,max}$ (MPa)	Δn ($\cdot 10^{-6}$)	δ (rad)
Uppermost	0.65	0.45	0.22	2.6	3.3
Lat. high	0.66	0.47	0.26	2.6	3.3
Lat. low	0.77	0.65	0.43	2.6	3.3
Lowermost	0.87	0.86	0.34	2.6	3.3

to the difference between the first and second principal stresses, results always positive: this means that the refractive index along the first principal direction is greater than that parallel to the second principal one, and the latter therefore represents the propagation fast axis. On the basis of the Mueller theory,[13] which provides the most general description of the interaction between light and optical elements in terms of polarization, each lens can be seen as a wave-plate, namely as a phase retarder which can be considered linear (at least in a first-order approximation). Therefore, the entity of the phase retardation (and hence of the polarization) induced between the principal directions can be described by the following matrix:

$$M_\delta(\theta) = \begin{pmatrix} 1 & 0 & 0 & 0 \\ 0 & \cos^2(2\theta) + \sin^2(2\theta)\cos(\delta) & \cos(2\theta)\sin(2\theta)(1-\cos(\delta)) & \sin(2\theta)\sin(\delta) \\ 0 & \cos(2\theta)\sin(2\theta)(1-\cos(\delta)) & \sin^2(2\theta) + \cos^2(2\theta)\cos(\delta) & -\cos(2\theta)\sin(\delta) \\ 0 & -\sin(2\theta)\sin(\delta) & \cos(2\theta)\sin(\delta) & \cos(\delta) \end{pmatrix}, \tag{19}$$

where θ represents the angle of the fast axis (the latter coincident with the second principal direction in such a context) with respect to the X axis. On the basis of Eq. (19) and Fig. 12, we can state that the lenses central portion behaves such as an attenuation filter, characterized by little retardation and transmission given by $\cos(\delta)$ for $\delta < 0.1$ rad; departing from the center, the phase difference starts to increase, the polarization becomes elliptical ($0.1 \text{ rad} < \delta < 1.57$ rad), then changes to purely circular polarization ($\pi/2$ rad phase difference), hence to elliptical and eventually linear polarization again, but perpendicular to the central polarization (π rad phase retardation) along the lenses edges. The latter birefringence state concerns the entire perimeter of the circular lenses, and a limited portion of the five edges for the pentagonal ones. Furthermore, the numerical computations demonstrate that the fast axis angle is comprised between $\pi/2$ rad (at the center) and $3/4\pi$ rad (at the edges): the maximum crosstalk between the Stokes parameters, limiting the maximum achievable accuracy, is then given by $|\sin(\delta)|$ for the single lens.

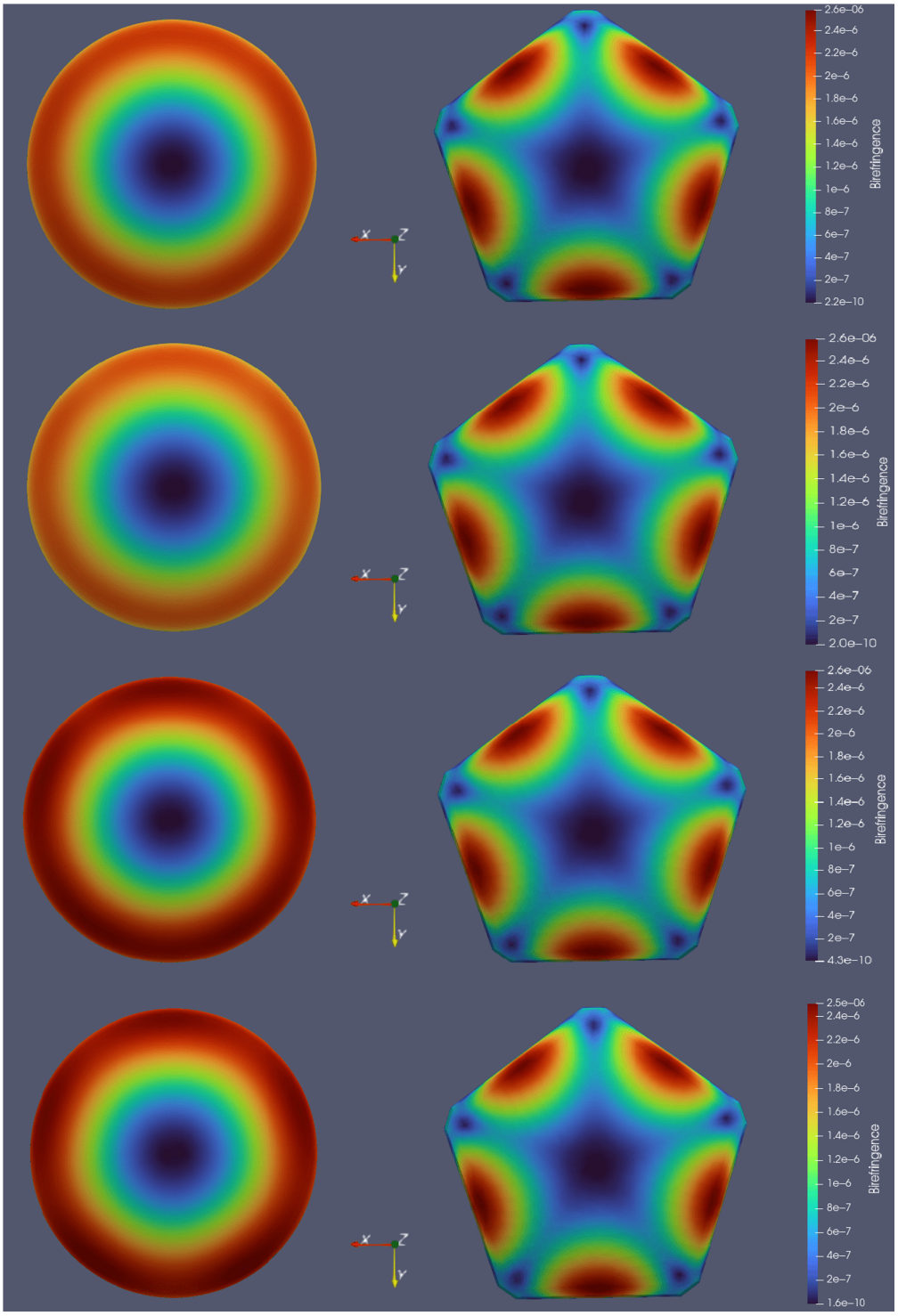

(a) (b)

Fig. 11 Refractive index difference between the first and second principal directions for the MezzoCielo lenses. From the top: uppermost, upper hemisphere, lower hemisphere, and lowermost lenses. (a) Circular lenses and (b) pentagonal lenses.

However, because the light must cross two specular glass elements, rotated of π rad relative to each other in the dodecahedral structure, the overall Mueller matrix becomes $M_\delta(\theta)M_\delta(\theta+\pi)$: the total retardation tends hence to zero and the light can cross the instrument without significant change in the polarization status.

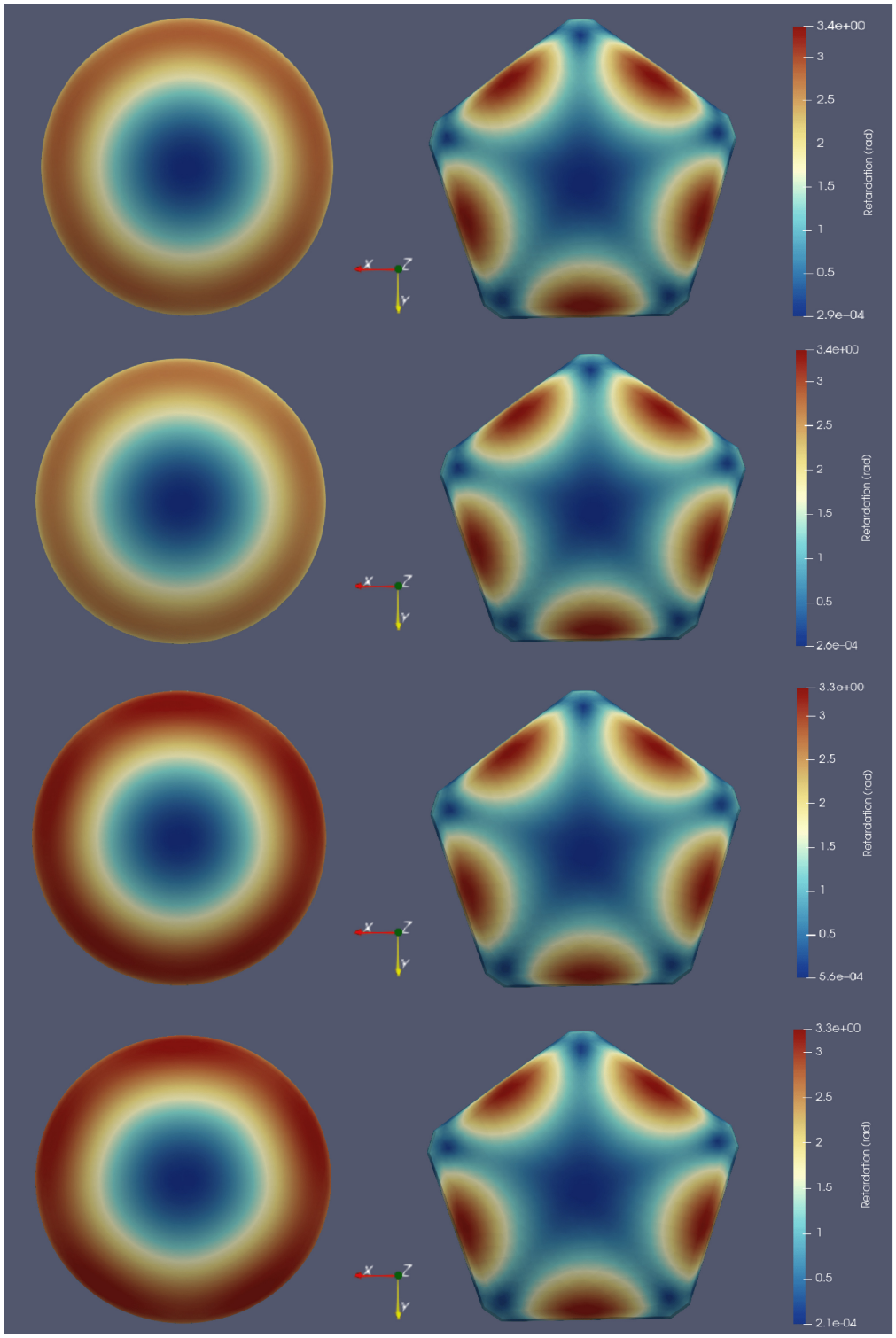

(a) (b)

Fig. 12 Phase retardation (in rad) between the first and second principal directions for the MezzoCielo lenses. From the top: uppermost, upper hemisphere, lower hemisphere, and lowermost lenses. (a) Circular lenses and (b) pentagonal lenses.

5 Conclusions

In this paper, the thermo-mechanical sizing of the MezzoCielo telescope structure has been described.

On the basis of geometrical and optical considerations, employed as starting point, the telescope optimal design has been chosen to be a dodecahedral one. The foreseen gravitational loads have been used to compute the expected lenses radius of curvature changes, and it has been verified that the desired radius tolerances (for high-quality optics) are greater than the load-induced displacements. Such considerations apply to both pentagonal and circular lenses.

In addition, the (supposed) environmental conditions during the winter activity have been chosen to size the telescope frame with the objective to minimize the thermal gradients between the instrument components (glass optics, metallic frame, and adhesives). Indeed, several finite element analysis have shown that the combination of both thermal and mechanical loads is much more severe, in terms of stresses, with respect to the only gravitational ones: safety factors and displacements have been therefore estimated in such worst-case scenario. The results are promising because they confirm the frame robustness and rigidity.

Eventually, the principal stresses within the lenses (both circular and pentagonal in shape) have been estimated and employed to compute the amount of birefringence (in terms of refractive index difference and phase retardation). The result was the achievement of a retardation map for each lens: on the basis of the Mueller theory, it has been deduced that the phase retardation (comprises between 0 and $\lambda/2$ for the single lens) tends to zero when two specular lenses are crossed in sequence.

In summary, it has been verified that the pentagonal lenses exhibit a lesser amount of displacements and stresses with respect to the circular ones, given the same boundary conditions; moreover, their birefringence is located mainly in a limited area around the edges, while the circular lenses birefringence occupies a significant portion of the clear aperture; finally, employing pentagonal lenses would allow reducing the obstruction produced by the metallic frame, for the benefit of the amount of gathered light and, therefore, limiting magnitude of the observable objects and resolution.

These advantages are counterbalanced by the increased manufacturing complexity and cost related to the realization of pentagonal lenses respect to "more standard" circular ones. Indeed, the abovementioned perks can be obtained only for pentagonal lenses properly made, namely characterized by a suitable degree of beveling, in particular near the vertices and the adjacent sharp edges.

The final choice regarding the MezzoCielo lenses shape should be made after the execution of tests on optical and mechanical bench, prepared to validate the results presented in this work.

Disclosures

The authors declare no conflicts of interest.

Code and Data Availability

The data that support the findings of this article are not publicly available due to privacy. They can be requested from the author at silvio.dirosa@inaf.it.

Acknowledgments

The first author of this paper wishes to express his gratitude to the co-authors and, in general, to all the colleagues who have supported his work with suggestions, advice, and criticism, in particular, the first author's supervisor, Roberto Ragazzoni, for having provided the guidelines of the entire project. A special thanks also to the University of Padua (Unipd) and the Italian Institute for Astrophysics (INAF) for the provided funding. A brief description of the topics covered in this work can be retrieved in the proceeding SPIE, S. D. Rosa, R. Ragazzoni, M. Dima et al., "Thermo-mechanical design and birefringence analysis for the MezzoCielo assembly", in Ground-based and Airborne Telescopes X, Japan 2024.

References

1. R. Ragazzoni et al., "Current status of MezzoCielo: a design aiming to a large aperture, extremely wide field of view telescope," *Proc. SPIE* **12182**, 121820H (2022).
2. S. D. Rosa et al., "Fluorine fluids experimental determination of the refractive index spectral and thermal variation and transparency quantification for the MezzoCielo telescope," *Opt. Mat. Express* **14**, 2542–2561 (2024).
3. S. D. Rosa et al., "Finite element analysis of the MezzoCielo monocentric optical system and other mechanical issues," *Proc. SPIE* **12182**, 121823S (2022).
4. S. Timoshenko, *Strength of materials, Part II, advanced theory and problems*, 3rd ed., D. Van Nostrand Company, Princeton, New Jersey (1956).
5. SCHOTT, "Optical glass datasheet schott n-bk7," Schott Company, https://www.schott.com/shop/advanced-optics/en/Optical-Glass/N-BK7/c/glass-N-BK7 (accessed 1 December 2023).
6. INAF, "Mount ekar observing station," Astronomical Observatory of Padua, https://web.oapd.inaf.it/meteo-ekar/archive.php (accessed May 2024).
7. SCHOTT, "Tie 19: temperature coefficient of the refractive index," Schott Company, Technical Information Advanced Optics, 2023, https://www.schott.com/en-th/products/optical-glass-p1000267/downloads.
8. P. L. Yoder, *Opto-mechanical systems design*, 3rd ed., CRC Press, Taylor & Francis Group, New York (2006).
9. C. T. Corporation, "Kovar technical data," High Temp Metals, 2015, https://www.hightempmetals.com/techdata/hitempKovardata.php.
10. SCHOTT, "Tie 33: bending strength of optical glass and Zerodur," Schott Company, Technical Information Advanced Optics, 2015, https://www.us.schott.com/shop/advanced-optics/en/Optical-Glass/SCHOTT-N-BK7/c/glass-SCHOTT.
11. M. Born and E. Wolf, *Principles of optics*, 7th ed., Cambridge University Press, Cambridge, United Kingdom (1999).
12. R. M. Anche et al., "Stress-induced birefringence in the lenses of wide-area linear optical polarimeter-south," *Proc. SPIE* **12188**, 121882C (2022).
13. M. Bass, *Handbook of optics, Vol. 1: geometrical and physical optics, polarized light, components and instruments*, 3rd ed., McGraw Hill, New York (2010).

Silvio Di Rosa is a PhD student at the University of Padua in Italy. He received his BS and MS degrees in mechatronics and aerospace engineering from the University of Padua in 2017 and 2020, respectively. Thanks to the publication of his master thesis on the opto-mechanical sizing of large optical systems, he achieved a PhD fellowship in astronomy. In addition, he attended a Master in Space Technology at the University of Bologna. Since 2021, he collaborates with the Italian Institute for Astrophysics (INAF) for the realization of large optical systems. He is a member of SPIE.

Biographies of the other authors are not available.